Science Advances

AAAS

advances.sciencemag.org/cgi/content/full/3/12/eaao4641/DC1

Supplementary Materials for

Nanoscale magnetic imaging using circularly polarized high-harmonic radiation

Ofer Kfir, Sergey Zayko, Christina Nolte, Murat Sivis, Marcel Möller, Birgit Hebler, Sri Sai Phani Kanth Arekapudi, Daniel Steil, Sascha Schäfer, Manfred Albrecht, Oren Cohen, Stefan Mathias, Claus Ropers

Published 15 December 2017, *Sci. Adv.* **3**, eaao4641 (2017)
DOI: 10.1126/sciadv.aao4641

This PDF file includes:

- fig. S1. Diffraction patterns for left- and right-handed circularly polarized HHG for the reconstructions presented in Figs. 2 and 3.
- fig. S2. Azimuthally averaged PRTF for the data presented in Figs. 2 and 3.
- fig. S3. Amplitude and phase maps to complement the phase images in Fig. 2.
- fig. S4. The reconstructed wave exiting the reference holes, partly presented in Fig. 2F.
- References (*54*, *55*)

Supplementary Materials

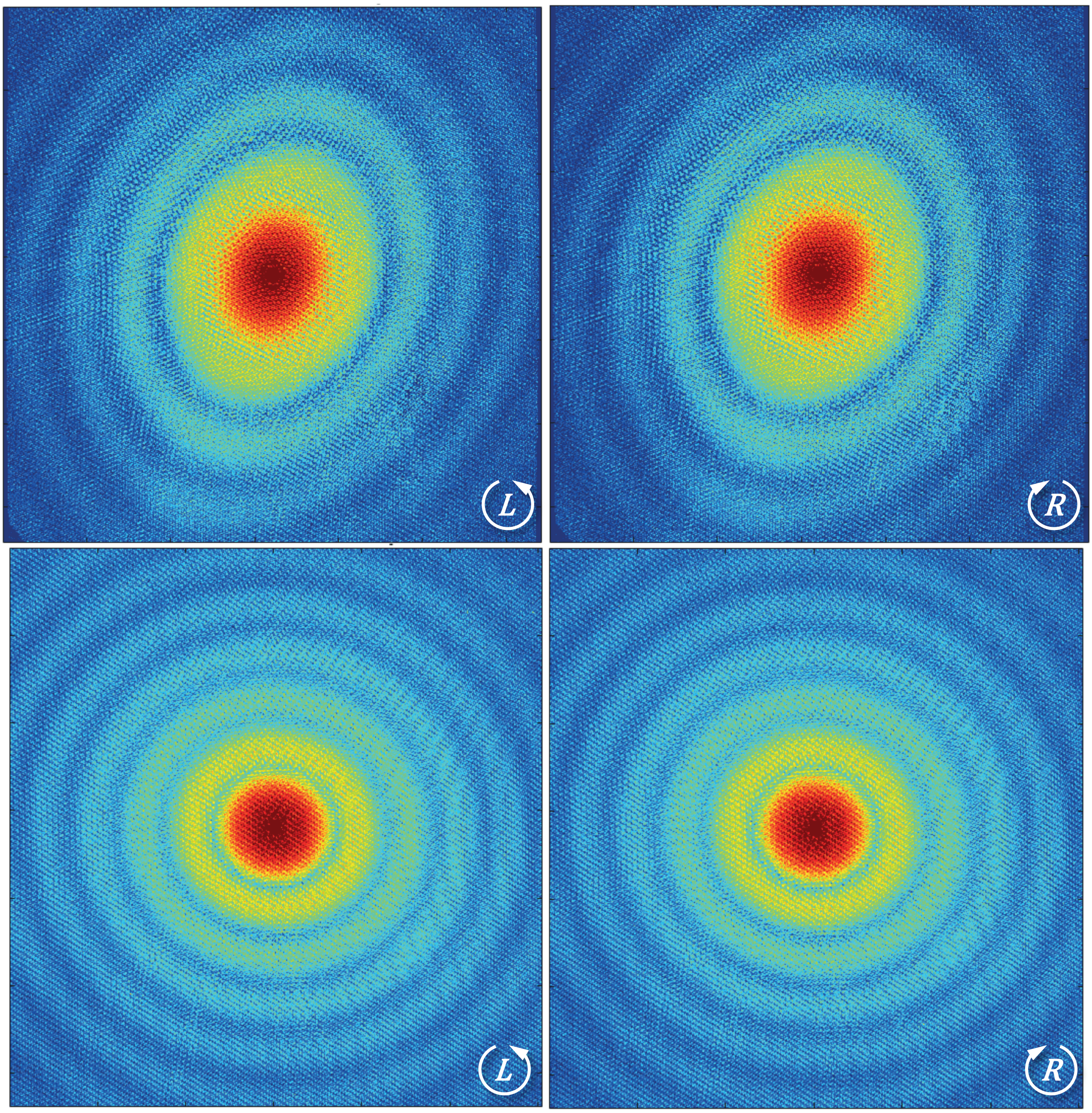

fig. S1. Diffraction patterns for left- and right-handed circularly polarized HHG for the reconstructions presented in Figs. 2 and 3. The difference between diffractions recorded with opposing polarization is hardly noticeable due to the weak magneto-optical scattering, compared with the non-dichroic scattering from the reference holes.

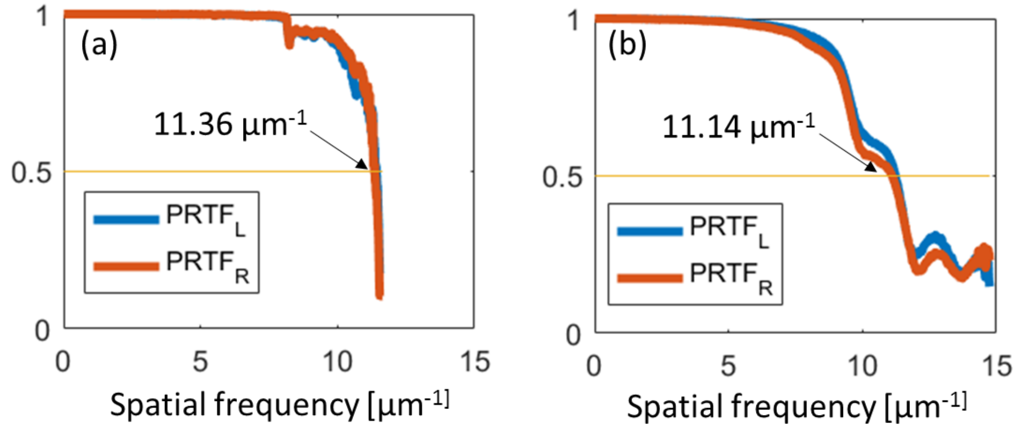

fig. S2. **Azimuthally averaged PRTF for the data presented in Figs. 2 and 3.** The PRTF is larger than 0.5 for spatial frequencies up to 11.36 µm-1 and 11.14 µm-1, corresponding to a spatial resolutions of 44 nm and 45 nm, respectively.

Holographic reconstruction

The complex wave exiting the sample can be written as a superposition of those from the central aperture and the reference holes

$$f_{exit}(\vec{r}) = f_{obj}(\vec{r}) + \sum_l f_{ref,l}(\vec{r} - \vec{r}_l)$$

Here, $\vec{r}$ is the two-dimensional radius vector in the sample plane, $f_{obj}(\vec{r})$ is the exit wave of the central aperture, and $l = 1,2,3,4$ is an index denoting the reference holes, where $\vec{r}_l$ and $f_{ref,l}(\vec{r} - \vec{r}_l)$ indicate the position and the exit wave of reference hole l, respectively. In the far-field (Fraunhofer approximation (*54*)), the intensity distribution measured by the CCD is given by

$$I_{CCD} \propto \left|FT\left[f_{obj}(\vec{r})\right]\right|^2 + \left|\sum_l FT\left[f_{ref,l}(\vec{r} - \vec{r}_l)\right]\right|^2 + 2\sum_l Re\left[FT\left[f_{obj}(\vec{r})\right]\left(FT\left[f_{ref,l}(\vec{r} - \vec{r}_l)\right]\right)^*\right]$$

where FT is the two-dimensional Fourier transform. Thus, an inverse Fourier transform of this intensity pattern results in multiple reconstructions of the object's exit wave, one for every reference hole

$$f_{rec,l} = f_{obj}(\vec{r}) \otimes f^*_{ref,l}(-\vec{r} - \vec{r}_l) \approx f_{obj}(\vec{r} + \vec{r}_l)$$

where $\otimes$ denotes a convolution, and the final approximation corresponds to a point-like reference hole. Thus, the reconstruction of hole l is placed on the opposite side of its physical position on the sample. A conjugated image for hole l is given by $f_{conj,l} = f^*_{obj}(-\vec{r}) \otimes f_{ref,l}(\vec{r} - \vec{r}_l) \approx f^*_{obj}(-\vec{r} + \vec{r}_l)$

For completeness, fig. S3 (a) and (c) show the amplitude maps of the holographic and CDI reconstructions, respectively, corresponding to the phase images in Fig. 2 of the manuscript (reproduced in fig. S3 b and d).

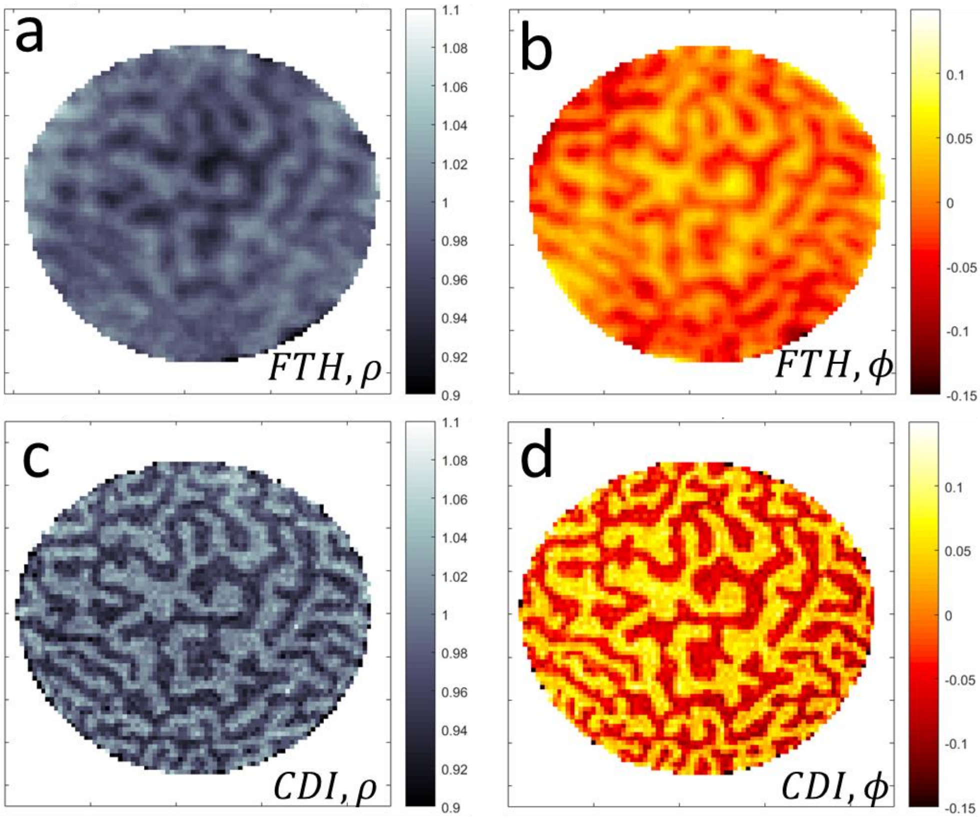

fig. S3. Amplitude and phase maps to complement the phase images in Fig. 2. Additional data for the reconstructions in Fig. 2. (a) Amplitude and (b) phase magneto-optical contrast images based on a single step FTH reconstruction. (c and d) Corresponding images for the CDI reconstruction. (b and d) are reproduced from fig. 2d and e of the manuscript.

Exit wave of the reference holes

Figure 2F in the manuscript presents the exit-wave of reference holes 1 and 2. For completeness fig. S4 shows the exit wave from all the reference holes as reconstructed, alongside images obtained using zero-padding in reciprocal-space, to stress the multi-modal nature of the waves exiting these holes. The pixel-scale variation of the exit-wave indicates that light is scattering to the edges of our CCD, where it interferes with and enhances the weak magneto-optical signal.

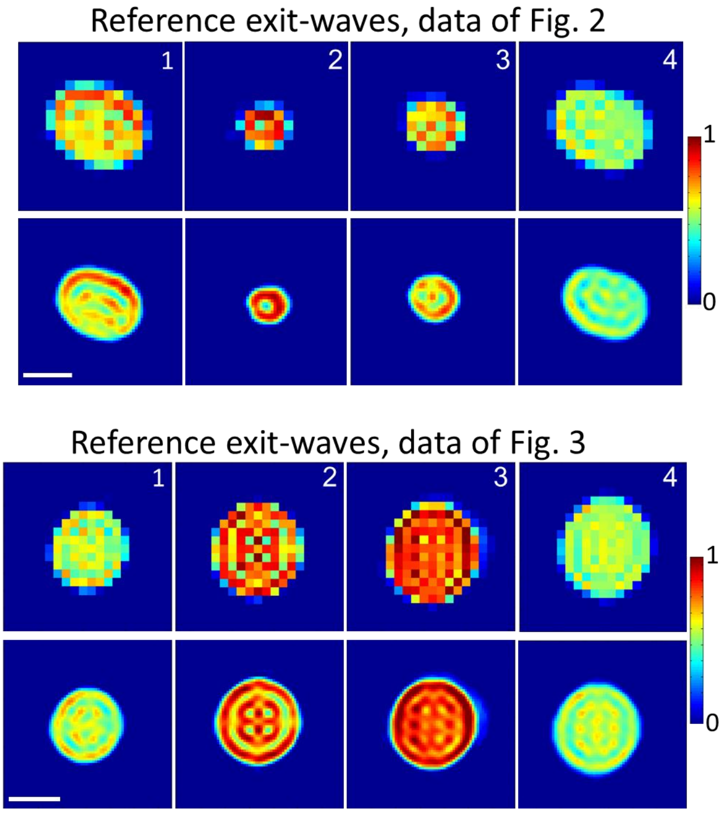

Fig. S4. The reconstructed wave exiting the reference holes, partly presented in Fig. 2F. As reconstructed (top row, numbered), and with zero-padding interpolation (second row). Scale-bars are 300 nm.

Notations for light helicity and magneto-optical interaction. For polarization helicities, we use a notation (*55*) in which the electric field of left-handed circular polarization is $\vec{E} \propto [\, \hat{x}\, cos(\omega t - kz) - \hat{y}\, sin(\omega t - kz)\,]$. $\hat{x}$ and $\hat{y}$ are the cartesian unit-vectors in the polarization plane, k is the wave number, ω is the angular frequency, t is time, and z is the position along the optical axis. For a given spatial wavefunction, $f(\vec{r})$, e.g., at the exit-plane of the sample, the physical electric field can be written in complex form as $\vec{E}_{L,R}(\vec{r}, t) = Re\left[E_0 \hat{e}_{L,R} e^{i\omega t} f(\vec{r})\right]$. Here, $\hat{r}$ is the 2-dimensional radius vector in the polarization plane. E_0 is the field's complex amplitude (including a constant phase), and $Re[\,]$ denotes the real part. L, R mark left-hand and right-hand circular polarization, with $\hat{e}_{L,R}$ as the normalized polarization vector, $\hat{e}_L = \frac{1}{\sqrt{2}}(\hat{x} + i\hat{y}),\ \hat{e}_R = \frac{1}{\sqrt{2}}(\hat{x} - i\hat{y})$.

As for the notation for the magneto-optical interaction, the term "parallel" magnetization is defined here differently than in the work by Valencia et al, (*32*). Note that we describe the magnetization as being parallel or antiparallel to the beam's propagation direction. In Ref. (*32*), "parallel" refers to the relation between the magnetization and the respective polarization helicity of the beam. These terminologies coincide for left-hand polarization.